Desalination and Water Treatment
www.deswater.com

doi: 10.5004/dwt.2019.24674

169 (2019) 38–48
November

Experimental design modelling and optimization of levofloxacin removal with graphene nanoplatelets using response surface method

Awais Zaka[a], Taleb H. Ibrahim[a,*], Mustafa I. Khamis[b], Nabil Abdel Jabbar[a]

[a]*Department of Chemical Engineering, American University of Sharjah, U.A.E, email: italeb@aus.edu (T.H. Ibrahim)*
[b]*Department of Biology, Chemistry and Environmental Sciences, American University of Sharjah, U.A.E*

Received 13 May 2019; Accepted 9 July 2019

ABSTRACT

A response surface modelling methodology was employed in this study to evaluate the effect of four different parameters for the removal of levofloxacin using graphene nanoplatelets. A quadratic statistical model was chosen to represent the process mathematically via an experimental design method. Analysis of variance showed that the mathematical model is in good agreement with the experimental data. The numerical optimization was performed to find the optimum values of process variables which were: contact time = 77 min, adsorbent dosage = 2.1 g L^{-1}, pH = 5.1 and initial concentration of levofloxacin = 10.7 mg L^{-1}. Adsorption experiments were conducted using these optimum parameters and the experimental data were fitted to different isotherms and kinetic models to study the behaviour of the adsorption process. It was observed that the adsorption of levofloxacin on graphene nanoplatelets follows Langmuir isotherm model (R^2 = 0.996 and K_L = 1.188 L mg^{-1}) and pseudo-second-order kinetics (R^2 = 0.999 and k_2 = 0.1407 g mg^{-1} min^{-1}). Thermodynamic properties were calculated through Sips equation, which indicated that the adsorption process is endothermic in nature.

Keywords: Adsorption; Graphene nanoplatelets; Levofloxacin; Response surface model

1. Introduction

Pharmaceuticals, due to their increasing demand and continuous production, have emerged as a new class of organic contaminants entering in the environment. The continual introduction to the environment and long-time persistence of these compounds have led to severe ecological effects on many species including human beings, fish and birds [1–4]. Antibiotics are the most commonly used pharmaceuticals [5]. These once released in the environment can lead to a serious toxic risk to different aquatic organisms [6].

Levofloxacin (LFX) is a popular antibiotic belonging to the class of fluoroquinolones (FQs). It is a 3rd generation quinolone especially active against both gram-positive and gram-negative bacteria [7,8]. The high consumption of quinolones has led to its frequent detection in wastewater [9]. These quinolones cannot be efficiently removed through conventional biological wastewater treatment techniques due to their poor biodegradability [10]. Because antibiotics are designed to kill the bacteria not being destroyed by the bacteria, a long-time exposure to antibiotics can result in the evolution of stronger antibacterial resistance in bacteria [11]. Moreover, FQ antibiotics can have an adverse effect on a cell's genetic material such as DNA and thus can prove to be genotoxic [12]. Hence, there is a need to develop a new and more efficient treatment method to reduce the possible effect of antibiotics on different species.

The inability of conventional wastewater treatment processes to remove pharmaceuticals has led to the invention of different other techniques such as advanced oxidation processes, Fenton oxidation, photo-degradation and other hybrid systems combining chemical and biological

* Corresponding author.

Presented at the Sixth International Conference on Water, Energy and Environment 2019 (ICWEE-2019), 26–28 March 2019, Sharjah, United Arab Emirates

techniques. However, the use of these methods is limited due to different disadvantages at various stages of operations [13]. Among these techniques, adsorption has emerged as an economical and operatively simple phenomenon that has proved to be efficient in removing pharmaceutical compounds from wastewater without producing toxic by-products [14,15].

Graphene, due to its unique two-dimensional structure and properties, has emerged as a promising material in research study. It has found many applications in sensors, hydrogen storage, electronics and nano-electronics [16,17]. High theoretical surface area of graphene promises its practical use in wastewater treatment especially in adsorption process and this is the reason that it has been used in the removal of several pollutants such as heavy metals, dyes and pharmaceuticals [16,18,19].

Response surface modelling (RSM) is a popular statistical tool that is used to study the effect of several independent variables on one or more response variables. The combination of several mathematical and statistical approaches in RSM is used for the improvement and optimization of processes and this is the reason that RSM technique finds its extensive use in industrial research [20,21]. The use of the RSM approach in wastewater treatment especially ones based on adsorption techniques has led to many advantages such as improved yield, cost optimization and process time reduction [22]. RSM technique has proved to be more useful than other methods because it does not only include the effect of different variables but also incorporates the interaction between them and hence depicts a comprehensive influence of all parameters [23].

In this work, the applicability of RSM technique for the removal of levofloxacin using graphene nanoplatelets (GNPs) is presented. A mathematical model was developed using central composite design (CCD) and its verification is presented.

2. Materials and methods

2.1. Materials

Pure samples of levofloxacin (LFX) ($C_{18}H_{20}FN_3O_4$, CAS No. 100986-85-4) was obtained from a local pharmaceutical company (Julphar Gulf Pharmaceutical Manufactures) in UAE and used without further purification. GNPs (99% purity) were purchased from Grafen Chemical Industries (Turkey). Scanning electron microscope (SEM) image shows the physical morphology of graphene used in the study (Fig. 1). The clear voids and cavities on the graphene surface are clear from the image. It has a surface area of 120–150 $m^2\ g^{-1}$, while density, diameter and thickness are 0.05 g cm^{-3}, 5–10 μm and 8 nm, respectively. Stock solution of LFX was prepared by dissolving a certain amount in distilled water. The stock solution was diluted with distilled water to obtain different concentrations. The solution pH was adjusted using 0.1 M aqueous solutions of either NaOH or HCl.

2.2. Instrumentation

A temperature-controlled multi-stack refrigerated shaking incubator (DAIHAN Scientific, South Korea) was used to control the temperature and the shaking rate of the adsorption experiments. The initial pH of the solutions was measured using Orion 210A+ basic pH meter (Thermo Electron Corporation, USA). The concentration of LFX was measured through UV–Vis spectrometer (Cary 50 Conc, Varian, Australia). The solutions were filtered using 4.5 μm syringe filters (Chrome Tech, Germany). Characterization of graphene was performed on a SEM (Tescan Vega3-lmu, USA).

2.3. Design of experiments

Design-Expert® Software (Version 11, Stat-Ease Inc., USA) was used to model the effect of the independent variables on the removal efficiency of LFX by GNP. The independent variables are contact time (A, min), adsorbent dosage (B, g L^{-1}), initial concentration of LFX (C, mg L^{-1}) and pH (D). For each parameter, five levels were studied as shown in Table 1. The low (–1) and high (+1) levels are the lower and upper value of the variables while the points at $\pm\alpha$ represent the axial points outside the response surface. Removal efficiency (Y, %) was the response variable in this study. CCD was applied to study the effects of above independent parameters on the response variable. CCD is a standard RSM design and is considered helpful in the optimization study with the minimum number of experimentations [24].

The total number of experiments was calculated according to Eq. (1).

$$N = 2^k + 2k + n_c \tag{1}$$

where N is the total number of experiments, k is the number of variables and n_c is the number of centre points. The first term in the above equation shows the number of experiments at factorial points while the second and third

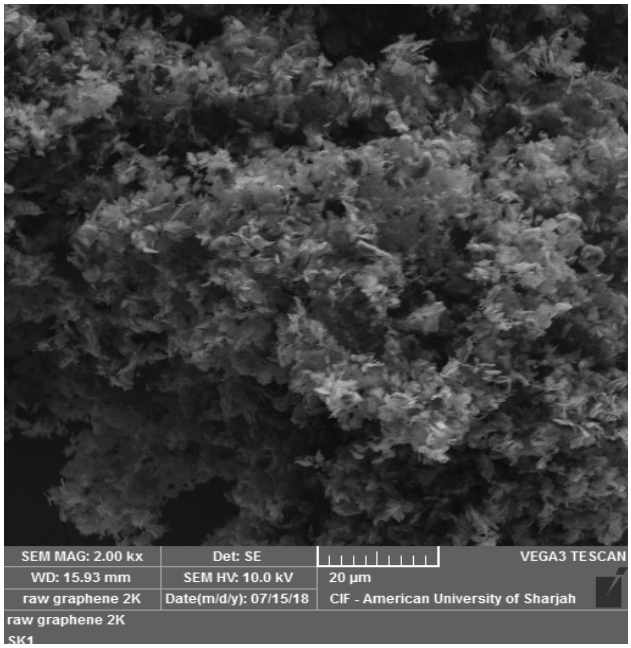

Fig. 1. SEM image for pure graphene.

Table 1
Range of variables and experimental levels

Factor			Levels		
	$-\alpha$	Low (–1)	Central (0)	High (+1)	$+\alpha$
A	30	100	170	240	310
B	0.25	1.0	1.75	2.50	3.25
C	5.0	10.0	15.0	20.0	25.0
D	2.5	5.0	7.5	10.0	12.5

terms give the number of experiments at axial and centre points, respectively. Hence, the total number of experiments calculated was 30 including 6 centre points. The LFX removal efficiency can be represented in mathematical form as:

$$Y = \beta_o + \sum_{i=1}^{k} \beta_i x_i + \sum_{i=1}^{k}\sum_{j=1}^{k} \beta_{ij} x_i x_j + \sum_{i=1}^{k} \beta_{ii} x_i^2 + \varepsilon \quad (2)$$

where Y represents the response variable, β_0 is the constant regression coefficient, β_i is the ith linear regression coefficient, β_{ii} is the ith quadratic coefficient, β_j is the interaction coefficient, x_i and x_j are the independent variables and ε is the residual error. The experimental results were used to perform regression analysis to fit the equation developed. The regression coefficient of determination (R^2) was used to determine the quality of fit of the polynomial model generated by the software.

2.4. Adsorption experiments

Batch adsorption experiments were conducted using the optimum condition as predicted by the model generated by the software. In a typical study, 10.0 mL LFX solution of known concentration was prepared by diluting stock solution in a 50 mL Erlenmeyer flask. A weighed amount of adsorbent was then added to the solution after the adjustment of pH. This solution was then placed in a shaking incubator at 25°C and agitated for a specified time at a speed of 150 rpm.

The adsorbent was separated from adsorbate using a syringe filter. The concentration of LFX was measured through UV–Vis spectrometer at a wavelength of 288.9 nm. A calibration curve was first obtained through the linear fitting (R^2 = 0.999) using known samples as shown in Fig. 2. Eq. (3) gives the regression equation for the dependence of the absorbance on concentration. The removal efficiency was calculated from Eq. (4).

$$A = 0.072x - 0.0086 \quad (3)$$

$$\text{Removal } \% = \frac{(C_0 - C_e)}{C_0} \times 100 \quad (4)$$

where A is the absorbance, x is the concentration of LFX (mg L^{-1}) and C_0 and C_e are the initial and final concentrations of LFX, respectively.

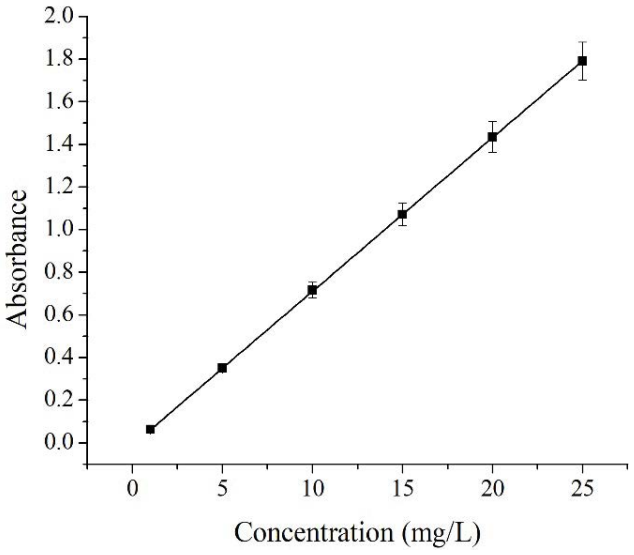

Fig. 2. Calibration curve for absorbance of different concentrations of levofloxacin measured at λ_{max} = 288.9 nm.

3. Results and discussion

3.1. Results from model

The CCD model was employed to construct a mathematical expression representing correlation between the percentage removal of LFX and the process variables. This method provided the coefficients of the best fitted variables that can be used to predict the values of the removal efficiencies using Eq. (5). Table 2 summarizes these predicted values together with the experimentally obtained response variable. Experiments from 25 to 30 represent the centre point runs used to calculate the true error. The best fitting model as suggested by the software was quadratic. The model is mathematically expressed in terms of actual variables and is given as follows:

$$Y = 58.93373 + 0.0445A + 42.590B - 4.970C + 6.263D - 0.003AB - 0.0012AC - 0.001AD + 1.729BC + 1.072BD + 0.272CD + \left(2\times10^{-6}\right)A^2 - 15.207B^2 - 0.045C^2 - 0.845D^2 \quad (5)$$

where *A*, *B*, *C* and *D* represents time, dosage of adsorbent, initial concentration of LFX and pH, respectively and *Y* represent the removal percentage of LFX after treating with GNP. Eq. (5) mathematically represents not only the effect of all four variables individually but also includes the effect arising due to the interaction of variables with each other. The actual and predicted values are represented in Fig. 3. The predicted regression coefficient value (R^2 = 0.8722) was found to be in good agreement with the adjusted value (R^2 = 0.9560).

3.2. Analysis of variance (ANOVA)

To verify the significance of quadratic model statistically, analysis of variance (ANOVA) was performed. The results from ANOVA are presented in Table 3. The results show that the employed model is significant. The model terms

Table 2
Design of experiments (DOE)

Standard sequence	Actual run sequence	Time	Dosage	Initial concentration	pH	% Removal (actual)	% Removal (predicted)
01	29	100	1	10	5	85.6	81.13
02	19	240	1	10	5	88.18	85.57
03	06	100	2.5	10	5	98.06	98.75
04	18	240	2.5	10	5	97.54	102.55
05	20	100	1	20	5	46.07	47.37
06	02	240	1	10	5	48.746	50.11
07	10	100	2.5	20	5	88.564	90.93
08	21	240	2.5	20	5	92.24	93.04
09	22	100	1	10	10	67.061	67.53
10	11	240	1	10	10	74.448	71.26
11	04	100	2.5	10	10	95.377	93.19
12	13	240	2.5	10	10	96.30	96.28
13	07	100	1	20	10	53.218	47.38
14	30	240	1	20	10	48.82	49.41
15	08	100	2.5	20	10	95.107	98.99
16	15	240	2.5	20	10	96.738	100.38
17	23	30	1.75	15	7.5	90.367	92.00
18	28	310	1.75	15	7.5	95.256	97.83
19	14	170	0.25	15	7.5	17.7	25.99
20	01	170	3.25	15	7.5	99.404	94.58
21	09	170	1.75	5	7.5	99.41	104.74
22	16	170	1.75	25	7.5	76.94	75.07
23	03	170	1.75	15	2.5	76.54	76.49
24	17	170	1.75	15	12.5	66.738	70.23
25	25	170	1.75	15	7.5	93.45	94.49
26	24	170	1.75	15	7.5	92.18	94.49
27	26	170	1.75	15	7.5	93.91	94.49
28	27	170	1.75	15	7.5	94.60	94.49
29	12	170	1.75	15	7.5	93.19	94.49
30	05	170	1.75	15	7.5	96.09	94.49

with p-values of <0.0001 are most significant. In this case it was found that the most significant variables were the dosage of adsorbent (B), initial concentration of LFX (C), combination of dosage and concentration (BC), combination of concentration and pH (CD), square of dosage (B^2) and pH (D^2). Details of ANOVA are given in Table 3.

3.3. Model prediction of the combined effect of design parameters

The individual effect of parameters under investigation on the efficiency of GNP for the removal of LFX is shown in Fig. 4. It can be observed that the effect of time remains almost the same for the whole range suggesting that the adsorption takes place quickly. The dosage of GNP has a very significant effect on the removal. The efficiency increases exponentially with an increase in the adsorbent dosage and a plateau is achieved at a dosage value of 2.2 g L^{-1}. An inverse relation is observed between the concentration of LFX and removal which can be attributed to the saturation of graphene surface with LFX molecules. The individual

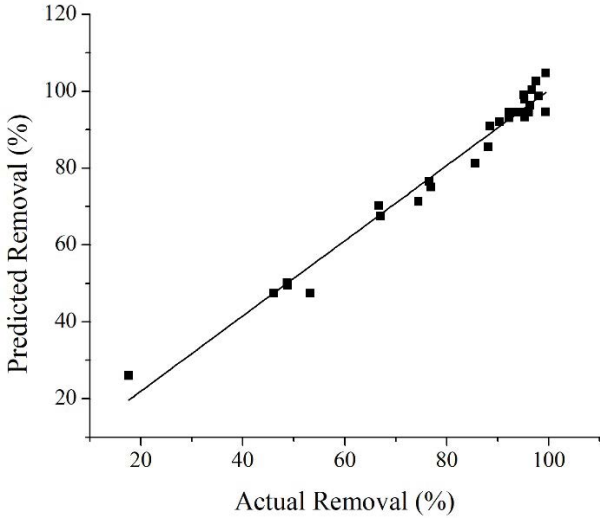

Fig. 3. Actual vs. predicted plot for LFX removal.

Table 3
Analysis of variance (ANOVA) for quadratic model

Source	Sum of squares	*df*	Mean square	*F*-value	*p*-value	Remarks
Model	11,933.24	14	852.37	46.04	<0.0001	Significant
A (time)	23.48	1	23.48	1.27	0.2778	
B (dosage)	7,044.51	1	7,044.51	380.47	<0.0001	Significant
C (LFX Concentration)	1,320.18	1	1,320.18	71.30	<0.0001	Significant
D (pH)	58.75	1	58.75	3.17	0.0951	
AB	0.4023	1	0.4023	0.0217	0.8848	
AC	2.88	1	2.88	0.1558	0.6986	
AD	0.5130	1	0.5130	0.0277	0.8700	
BC	673.39	1	673.39	36.37	<0.0001	Significant
BD	64.69	1	64.69	3.49	0.0813	
CD	185.39	1	185.39	10.01	0.0064	
A^2	0.0031	1	0.0031	0.0002	0.9898	
B^2	2,007.06	1	2,007.06	108.40	<0.0001	Significant
C^2	36.06	1	36.06	1.95	0.1831	
D^2	765.19	1	765.19	41.33	<0.0001	Significant
Residual	277.73	15	18.52			
Lack of fit	268.8	10	26.88	15.06	0.0040	
Pure error	8.92	5	1.78			
Corrections total	12,210.97	29				

df = Degree of freedom.
F-value: Test for comparison between residual mean square and source mean square.
p-value: Probability of having observed *F*-value if there are no factor effects. A *p*-value less than 0.05 reflects that the model terms have a real effect on the response.

effect of pH is also shown in Fig. 4. The efficiency slightly decreases at very acidic and very basic conditions; however, the change is not significant as observed from the ANOVA. Only the adsorbent dosage and adsorbate concentration were found to have a significant effect individually.

The combined effect of different design parameters through a three-dimensional response surface is shown in Fig. 5a shows the interactive effect of contact time and adsorbent dosage at constant pH and LFX concentration. It can be observed that the removal efficiency increases with an increase in dosage as well as time. The trend remains the same if one of the variables is kept constant. This is because an increase in dosage will lead to a greater number of available sites and hence the removal will increase. The change in removal due to dosage is more significant as compared with the effect due to change in time. Fig. 5b shows the combined impact of initial levofloxacin concentration and contact time while pH and GNP dosage remain constant. At any given time, an increase in concentration will lead to a decrease in removal efficiency, which could be associated with the saturation of active sites. In Fig. 5c, the combined effect of pH and time is shown at constant dosage and LFX concentration. It depicts that the removal is low at strong acidic and strong basic pH environment, which can be attributed to the change in surface charge of GNP at values around pH 4 [25]. The effect of LFX concentration and GNP dosage collectively is shown in Fig. 5d. The observed trend illustrates that the removal is lowest at high concentrations of LFX and low dosage of graphene. Figs. 5e and f shows the collective effect of pH with dosage and concentration, respectively, which further implies the same effect of the parameters as discussed earlier.

3.4. Optimization and validation

The optimum parameters were obtained through the software with the idea of making the process economical in terms of both cost and time. The theoretical optimum values of the independent variables thus obtained are contact time = 77 min, GNP dosage = 2.113 g L^{-1}, pH = 5.118 and LFX concentration = 10.7 mg L^{-1}. The predicted value of removal percentage obtained at these parameters is 99.679% and the desirability value is 1.000.

To validate the predicted value, five experiments were conducted at optimum conditions which are contact time = 77 min, GNP dosage = 2.1 g L^{-1}, pH = 5 and LFX concentration = 10.5 mg L^{-1}. The experimental results for the removal efficiency for these five experiments were 98.29%, 98.15%, 98.55%, 97.97% and 98.59%. These values were found to be in the range of the given confidence and hence are in good agreement with the values predicted by the model.

3.4.1. Isotherms

Three different isotherm models, namely Langmuir, Freundlich and Temkin [26,27], were used to fit the experimental data obtained after several runs at optimum conditions

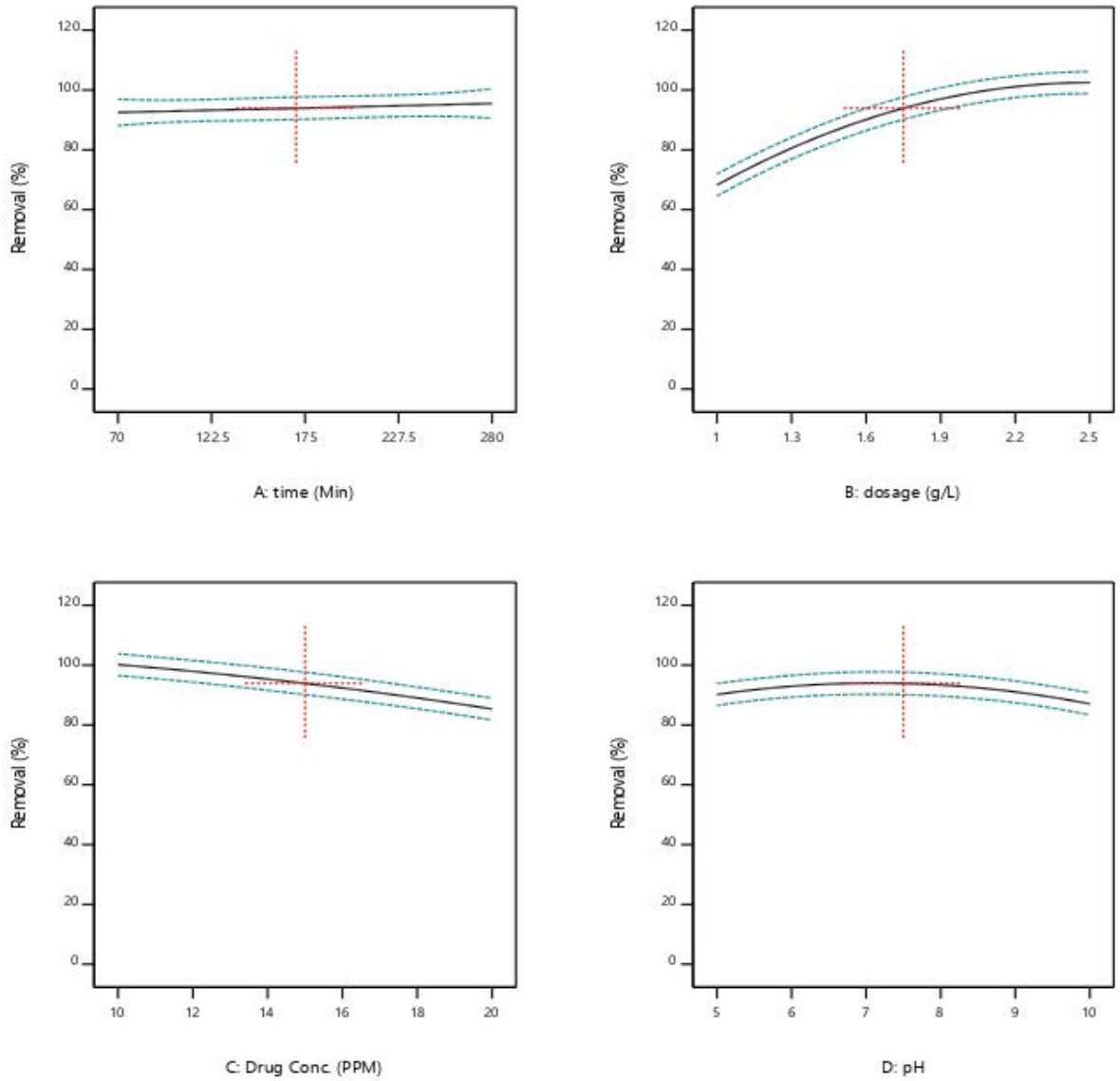

Fig. 4. Individual effect of different variables on the removal efficiency of levofloxacin.

of contact time, 10 and 30 mg L^{-1} and the equilibrium concentration (C_e) were measured for each experiment. The adsorption capacity at equilibrium (Q_e, mg g^{-1}) was calculated using Eq. (6) as follows:

$$Q_e = \frac{(C_0 - C_e)V}{m} \tag{6}$$

where m (g) is the mass of adsorbent and V (L) is the volume of the sample solution. The data were fitted to the linearized form of respective isotherms models as given by Eqs. (7)–(9).

$$\frac{C_e}{Q_e} = \frac{C_e}{Q_m} + \frac{1}{Q_m K_L} \tag{7}$$

$$\log Q_e = \log K_F + \frac{1}{n}\log C_e \tag{8}$$

$$Q_e = B \ln K_T + B \ln C_e \tag{9}$$

where Q_m (mg g^{-1}) is the maximum adsorption capacity of GNP, K_L (L mg^{-1}) is the Langmuir isotherm constant, K_F ($mg^{(1-1/n)}$ $L^{1/n}$ g^{-1}) and n are the Freundlich isotherm constants and B (J mol^{-1}) and K_T (L mg^{-1}) are the Temkin isotherm constants.

The values of regression coefficients for all isotherms obtained after data fitting along with other parameters are represented in Table 4. It can be observed that the adsorption of LFX is best described by the Langmuir isotherm model with and R^2 value of 0.996. This is an indication that the adsorption occurring is monolayer and homogeneous in nature. The plots of isotherms models are shown in Fig. 6.

3.4.2. Kinetics

Pseudo-first-order and pseudo-second-order kinetic models were used to fit the experimental model for the removal

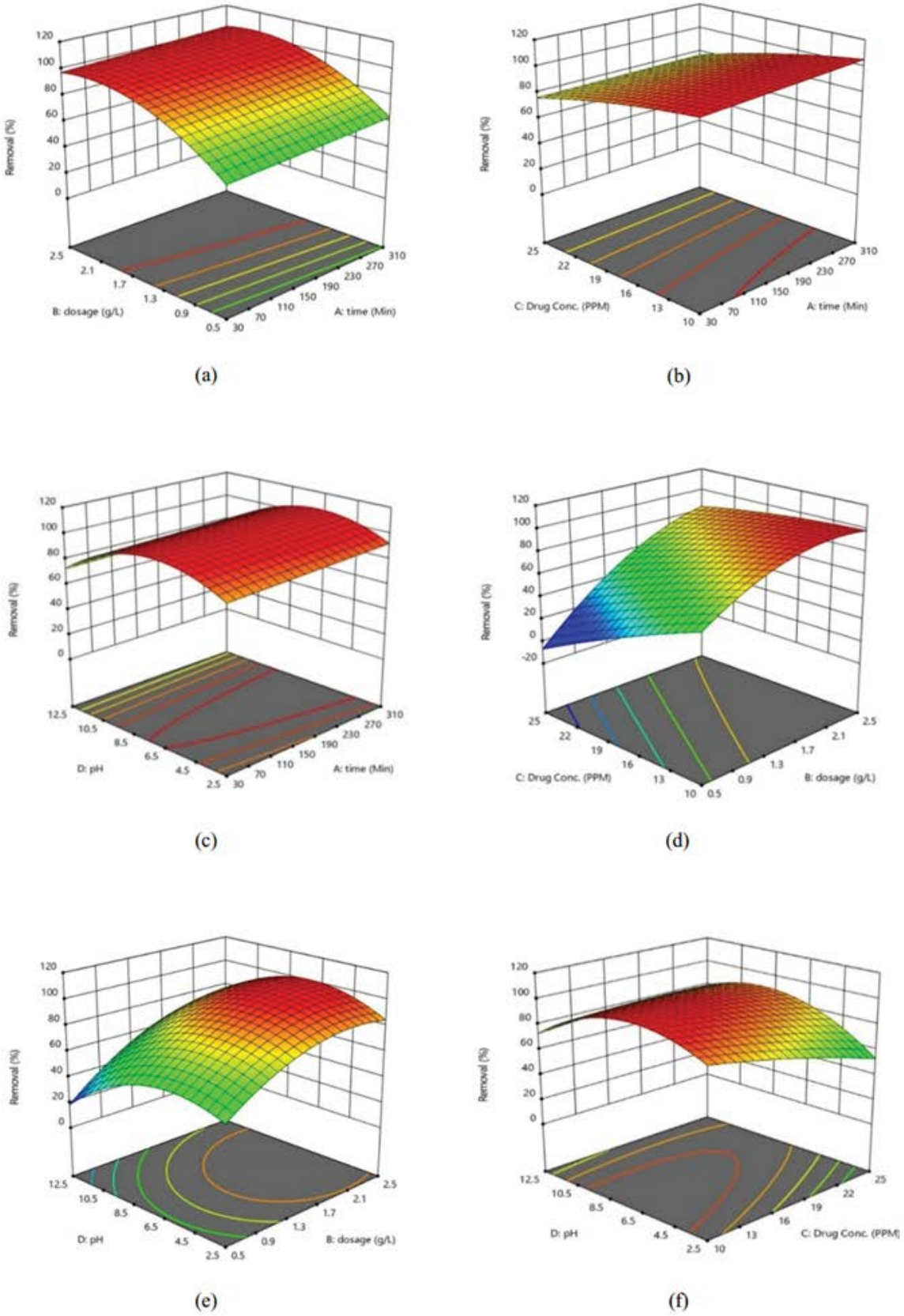

Fig. 5. 3D plots for LFX removal showing interaction between (a) dosage and time, (b) LFX concentration and time, (c) pH and time, (d) LFX concentration and dosage, (e) pH and dosage and (f) pH and LFX concentration.

of LFX using GNP. The linearized forms of respective models are given as follows:

$$\ln\left(Q_e - Q_t\right) = -k_1 t + \ln Q_e \tag{10}$$

$$\frac{t}{Q_t} = \frac{t}{Q_e} + \frac{1}{k_2 Q_e^2} \tag{11}$$

Table 4
Adsorption parameters for LFX removal

	Adsorption parameters	
Langmuir	K_L (L mg^{-1})	1.188 (±0.059)
	Q_m (mg g^{-1})	10.64 (±0.532)
	R^2	0.996
Freundlich	K_F (mg$^{(1-1/n)}$ L$^{1/n}$ g^{-1})	5.879 (±0.294)
	n	4.244 (±0.212)
	R^2	0.985
Temkin	B (J mol^{-1})	1.166 (±0.058)
	K_T (L mg^{-1})	38.07 (±1.903)
	R^2	0.994

where t (min) is the contact time between adsorbent and adsorbate, Q_t (mg g^{-1}) is the amount of LFX adsorbed at any time, k_1 (min^{-1}) and k_2 (g min^{-1} mg^{-1}) are the pseudo-first and pseudo-second-order rate constants. The plots for both kinetic models are shown in Fig. 7. Different parameters calculated from the graphs are summarized in Table 5. The observed R^2 value for pseudo-second-order model was found to be better than the 1 for pseudo-first-order model. The value of Q_e calculated from equation 11 (4.99 mg g^{-1}) was also close to the one found from equation 6 (4.69 mg g^{-1}). Hence, the conclusion can be made that the adsorption follows pseudo-second-order kinetics.

3.4.3. Thermodynamics

To investigate the energy changes associated with LFX removal, thermodynamic properties such as change in Gibbs free energy (ΔG), change in enthalpy (ΔH) and change in the entropy (ΔS) were calculated. The equation used to calculate ΔG is given as follows [28]:

$$G = -RT \ln K_{eq} \tag{12}$$

where R (J mol^{-1} K^{-1}) is the general gas constant, T (K) is the temperature and K_{eq} is the equilibrium constant. The value of

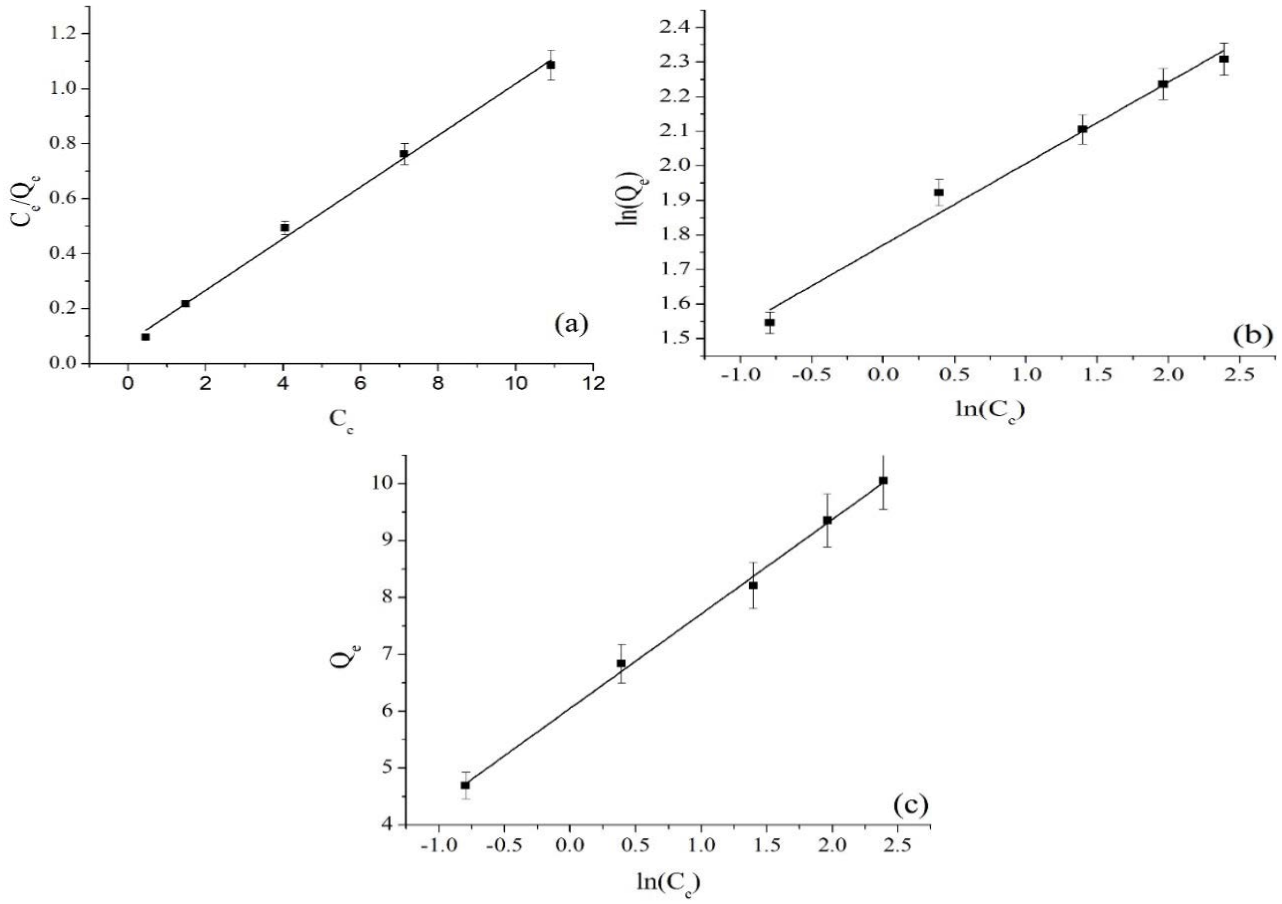

Fig. 6. Adsorption isotherm models for LFX removal. (a) Langmuir isotherm model, (b) Freundlich isotherm model and (c) Temkin isotherm model. Experimental conditions: shaker speed: 150 rpm; contact time = 80 min; initial pH = 5 ± 0.1; GNP dosage = 2 g L^{-1}; temperature = 25°C.

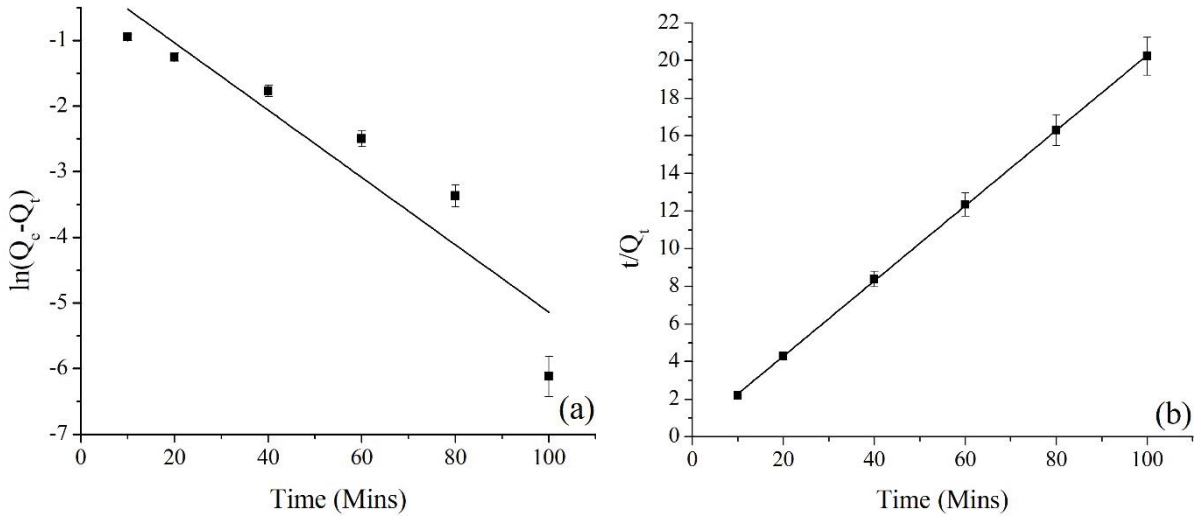

Fig. 7. Kinetic models for LFX removal (a) pseudo-first-order kinetic model and (b) pseudo-second-order kinetic model. Experimental conditions: shaker speed: 150 rpm; initial pH = 5 ± 0.1; GNP dosage = 2 g L^{-1}; initial concentration = 10.5 mg L^{-1}; temperature = 25°C.

Table 5
Kinetic model parameters for LFX removal

Model	Adsorption parameters	
Pseudo-first-order	k_1 (1 min^{-1})	0.051(±0.002)
	R^2	0.880
Pseudo-second-order	k_2 (g mg^{-1} min^{-1})	0.141(±0.007)
	R^2	0.999

Table 6
Calculated Sips parameters at different temperatures

Temperature (K)	K_{eq}	n_s	Q_e^{th} (mg g^{-1})
298.1	22.79 (±1.139))	0.235 (±0.011)	5.256 (±0.263)
308.1	26.33 (±1.316)	0.222 (±0.011)	3.802 (±0.190)
318.1	30.85 (±1.542)	0.235 (±0.011)	3.745 (±0.187)

the equilibrium constant was obtained through Sips equation [29–31]. The general form of Sips equation is given as [32]:

$$Q_e = Q_e^{th} \frac{C_e^{n_s}}{K_{ads}} \quad (13)$$

The value of Q_e^{th}, K_{ads} and n_s were calculated through regression analysis at various temperatures and are presented in Table 6. The equilibrium constant K_{eq} is then given as [30] follows:

$$K_{eq} = \frac{1}{K_{ads}} \quad (14)$$

The calculated values of ln (K_{eq}) were plotted against the inverse of temperature (1/T) in Van't Hoff plot as shown in Fig. 8. The apparent change in enthalpy (ΔH) and entropy (ΔS) can then be calculated through Van't Hoff equation, which is given as:

$$\ln K_{eq} = -\frac{\Delta H}{RT} + \frac{\Delta S}{R} \quad (15)$$

The calculated values of thermodynamic properties are shown in Table 7. It can be observed that the values of change in free energy range between –20 and 0 kJ mol^{-1}. This concludes that the adsorption of LFX on GNPs is

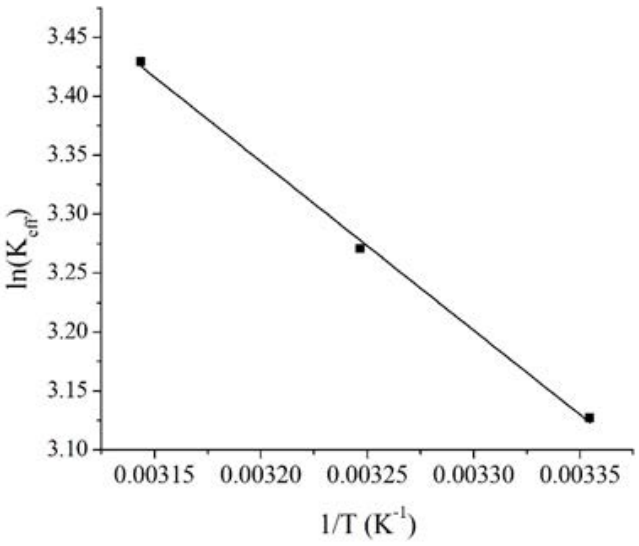

Fig. 8. Van't Hoff plot for LFX removal.

physical in nature [33]. Moreover, the negative sign indicates that the process is spontaneous. Furthermore, the increase in Gibbs free energy depicts that the adsorption is less feasible at elevated temperatures [25]. The negative slope of Van't' Hoff plot and positive sign of enthalpy change (ΔH) suggest that the process is endothermic in nature. Additionally, the positive value of entropy is associated with high affinity of

Table 7
Thermodynamic properties

ΔG			ΔH	ΔS
kJ mol^{-1}			kJ mol^{-1}	J mol^{-1} K^{-1}
298.1 K	308.1 K	318.1 K		
–7.748 (±0.3874)	–8.378 (±0.419)	–9.068 (±0.453)	11.92 (±0.595)	65.938 (±3.296)

sorbent for sorbate and means that there is an increase in the randomness at solid/liquid interface [25,34].

4. Conclusions

The removal efficiency of LFX by GNP was studied and the optimized parameters were obtained through RSM. CCD technique was used to study the effect of four independent parameters which are contact time, GNP dosage, pH and initial concentration of LFX. The process optimization revealed that the optimum conditions are contact time 77 min, GNP dosage 2.13 g L^{-1}, pH 5.11 and initial LFX concentration 10.5 mg L^{-1}. RSM and experimental findings were found to be in good agreement with each other. Langmuir isotherm model was the best-fit model for the adsorption process. Kinetic study showed that the adsorption follows pseudo-second-order model. Thermodynamic study showed that the process is spontaneous and endothermic.

Acknowledgements

The authors would like to thank Julphar Gulf Pharmaceutical Manufacturers UAE for providing the samples of levofloxacin for this study.

References

[1] M.J. Benotti, R.A. Trenholm, B.J. Vanderford, J.C. Holady, B.D. Stanford, S.A. Snyder, Pharmaceuticals and endocrine disrupting compounds in U.S. drinking water, Environ. Sci. Technol., 43 (2008) 597–603.
[2] N.J. Niemuth, R.D. Klaper, Emerging wastewater contaminant metformin causes intersex and reduced fecundity in fish, Chemosphere, 135 (2015) 38–45.
[3] J.L. Oaks, M. Gilbert, M.Z. Virani, R.T. Watson, C.U. Meteyer, B.A. Rideout, H.L. Shivaprasad, S. Ahmed, M.J.I. Chaudhry, M. Arshad, S. Mahmood, A. Ali, A.A. Khan, Diclofenac residues as the cause of vulture population decline in Pakistan, Nature, 427 (2004) 630–633.
[4] M. Hampel, E. Alonso, I. Aparicio, J.E. Bron, J.L. Santos, J.B. Taggart, M.J. Leaver, Potential physiological effects of pharmaceutical compounds in Atlantic salmon (*Salmo salar*) implied by transcriptomic analysis, Environ. Sci. Pollut. Res., 17 (2010) 917–933.
[5] P.K. Jjemba, Pharma-Ecology: The Occurrence and Fate of Pharmaceuticals and Personal Care Products in the Environment, John Wiley & Sons, United States of America, 2008.
[6] Y. Luo, L. Xu, M. Rysz, Y. Wang, H. Zhang, P.J. Alvarez, Occurrence and transport of tetracycline, sulfonamide, quinolone, and macrolide antibiotics in the Haihe River Basin, China, Environ. Sci. Technol., 45 (2011) 1827–1833.
[7] D. Nasuhoglu, A. Rodayan, D. Berk, V. Yargeau, Removal of the antibiotic levofloxacin (LEVO) in water by ozonation and TiO_2 photocatalysis, Chem. Eng. J., 189 (2012) 41–48.
[8] M. Ferech, S. Coenen, S. Malhotra-Kumar, K. Dvorakova, E. Hendrickx, C. Suetens, H. Goossens, ESAC Project Group, European Surveillance of Antimicrobial Consumption (ESAC): outpatient quinolone use in Europe, J. Antimicrob. Chemother., 58 (2006) 423–427.
[9] A.K. Sarmah, M.T. Meyer, A.B.A. Boxall, A global perspective on the use, sales, exposure pathways, occurrence, fate and effects of veterinary antibiotics (VAs) in the environment, Chemosphere, 65 (2006) 725–759.
[10] K. Kümmerer, A. Al-Ahmad, V. Mersch-Sundermann, Biodegradability of some antibiotics, elimination of the genotoxicity and affection of wastewater bacteria in a simple test, Chemosphere, 40 (2000) 701–710.
[11] F. Baquero, Low-level antibacterial resistance: a gateway to clinical resistance, Drug Resist. Updates, 4 (2001) 93–105.
[12] J. Hu, W. Wang, Z. Zhu, H. Chang, F. Pan, B. Lin, Quantitative structure-activity relationship model for prediction of genotoxic potential for quinolone antibacterials, Environ. Sci. Technol., 41 (2007) 4806–4812.
[13] J. Wang, S. Wang, Removal of pharmaceuticals and personal care products (PPCPs) from wastewater: a review, J. Environ. Manage., 182 (2016) 620–640.
[14] L.A. Al-Khateeb, S. Almotiry, M.A. Salam, Adsorption of pharmaceutical pollutants onto graphene nanoplatelets, Chem. Eng. J., 248 (2014) 191–199.
[15] S.-W. Nam, C. Jung, H. Li, M. Yu, J.R.V. Flora, L.K. Boateng, N. Her, K.-D. Zoh, Y. Yoon, Adsorption characteristics of diclofenac and sulfamethoxazole to graphene oxide in aqueous solution, Chemosphere, 136 (2015) 20–26.
[16] Y. Leng, W. Guo, S. Su, C. Yi, L. Xing, Removal of antimony(III) from aqueous solution by graphene as an adsorbent, Chem. Eng. J., 211 (2012) 406–411.
[17] Q. Liu, J. Shi, L. Zeng, T. Wang, Y. Cai, G. Jiang, Evaluation of graphene as an advantageous adsorbent for solid-phase extraction with chlorophenols as model analytes, J. Chromatogr. A, 1218 (2011) 197–204.
[18] X. Wang, B. Liu, Q. Lu, Q. Qu, Graphene-based materials: fabrication and application for adsorption in analytical chemistry, J. Chromatogr. A, 1362 (2014) 1–15.
[19] S. Wang, H. Sun, H.-M. Ang, M.O. Tadé, Adsorptive remediation of environmental pollutants using novel graphene-based nanomaterials, Chem. Eng. J., 226 (2013) 336–347.
[20] U.K. Garg, M.P. Kaur, V.K. Garg, D. Sud, Removal of Nickel(II) from aqueous solution by adsorption on agricultural waste biomass using a response surface methodological approach, Bioresour. Technol., 99 (2008) 1325–1331.
[21] R. Kumar, R. Singh, N. Kumar, K. Bishnoi, N.R. Bishnoi, Response surface methodology approach for optimization of biosorption process for removal of Cr (VI), Ni (II) and Zn (II) ions by immobilized bacterial biomass sp. *Bacillus brevis*, Chem. Eng. J., 146 (2009) 401–407.
[22] G. Annadural, R.S. Juang, D.J. Lee, Adsorption of heavy metals from water using banana and orange peels, Water Sci. Technol., 47 (2003) 185–190.
[23] D. Baş, İ.H. Boyacı, Modeling and optimization I: usability of response surface methodology, J. Food Eng., 78 (2007) 836–845.
[24] R. Azargohar, A.K. Dalai, Production of activated carbon from Luscar char: experimental and modeling studies, Microporous Mesoporous Mater., 85 (2005) 219–225.
[25] L.A. Chacra, M.A. Sabri, T.H. Ibrahim, M.I. Khamis, N.M. Hamdan, S. Al-Asheh, M. AlRefai, C. Fernandez, Application of graphene nanoplatelets and graphene magnetite for

the removal of emulsified oil from produced water, J. Environ. Chem. Eng., 6 (2018) 3018–3033.
[26] A.A. Inyinbor, F.A. Adekola, G.A. Olatunji, Kinetics, isotherms and thermodynamic modeling of liquid phase adsorption of Rhodamine B dye onto *Raphia hookerie* fruit epicarp, Water Resour. Ind., 15 (2016) 14–27.
[27] A.O. Dada, A.P. Olalekan, A.M. Olatunya, O. Dada, Langmuir, Freundlich, Temkin and Dubinin–Radushkevich isotherms studies of equilibrium sorption of Zn^{2+} unto phosphoric acid modified rice husk, IOSR J. Appl. Chem., 3 (2012) 38–45.
[28] P.S. Kumar, R. Gayathri, C. Senthamarai, M. Priyadharshini, P.S.A. Fernando, R. Srinath, V.V. Kumar, Kinetics, mechanism, isotherm and thermodynamic analysis of adsorption of cadmium ions by surface-modified *Strychnos potatorum* seeds, Korean J. Chem. Eng., 29 (2012) 1752–1760.
[29] Y. Liu, H. Xu, Equilibrium, thermodynamics and mechanisms of Ni^{2+} biosorption by aerobic granules, Biochem. Eng. J., 35 (2007) 174–182.
[30] Y. Liu, Y.-J. Liu, Biosorption isotherms, kinetics and thermodynamics, Sep. Purif. Technol., 61 (2008) 229–242.
[31] Y. Liu, Is the free energy change of adsorption correctly calculated?, J. Chem. Eng. Data, 54 (2009) 1981–1985.
[32] T.H. Ibrahim, M.A. Sabri, M.I. Khamis, Application of multi-walled carbon nanotubes and its magnetite derivative for emulsified oil removal from produced water, Environ. Technol., 10 (2018) 1–14.
[33] Y. Yu, Y.-Y. Zhuang, Z.-H. Wang, Adsorption of water-soluble dye onto functionalized resin, J. Colloid Interface Sci., 242 (2001) 288–293.
[34] N.P. Sotirelis, C.V. Chrysikopoulos, Interaction between graphene oxide nanoparticles and quartz sand, Environ. Sci. Technol., 49 (2015) 13413–13421.